Supplementary Information

Flexible and Stretchable Chromatic Fibers with High Sensing Reversibility

Xin Lu, Zhidong Zhang, Xuemei Sun, Peining Chen, Jing Zhang, Hui Guo, Zhengzhong Shao* and Huisheng Peng*

State Key Laboratory of Molecular Engineering of Polymers, Department of Macromolecular Science, and Laboratory of Advanced Materials, Fudan University, Shanghai 200438, China; E-mail: sunxm@fudan.edu.cn, zzshao@fudan.edu.cn.

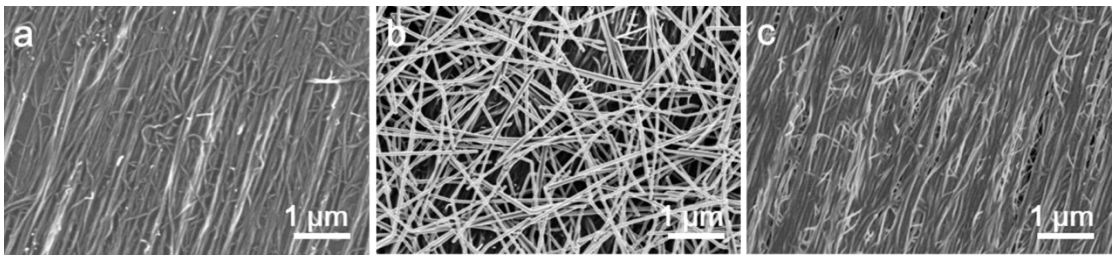

Fig. S1 SEM images of the surface of the conductive fiber during preparation. **a.** The inner CNT layer. **b.** The middle silver nanowire. **c.** The outer CNT layer.

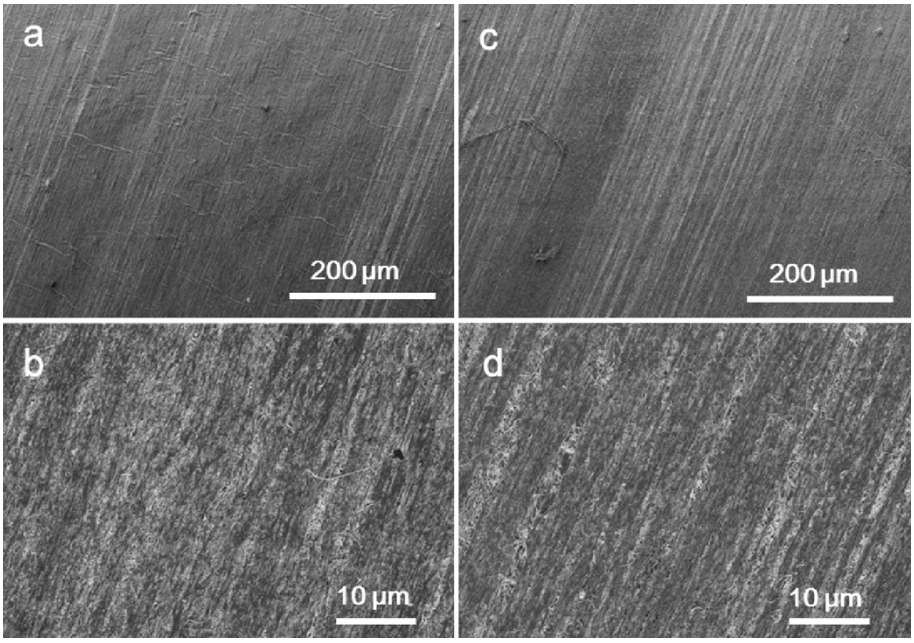

Fig. S2 SEM images of the elastic conductive fiber after stretching at different magnifications. **a** and **b.** Original state without stretching. **c** and **d.** After stretching (strain of 50%) for 1,000 cycles.

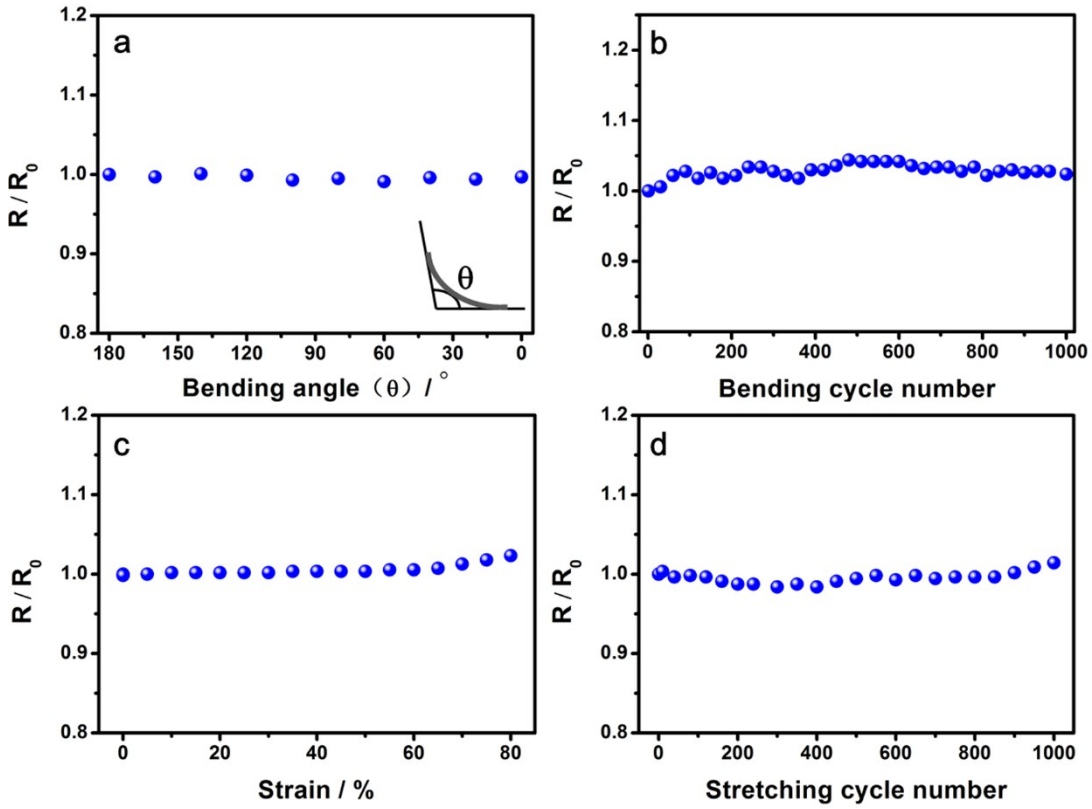

Fig. S3 Electrical property of the conductive fiber before and after bending or stretching. **a.** Dependence of resistance ratio on bending angle. **b.** Dependence of resistance on bending cycle number (with a bending angle of 90˚). **c.** Dependence of resistance ratio on strain. **d.** Dependence of resistance ratio on stretching cycle number (with a strain of 50%). Here R_0 and R correspond to the resistances before and after bending or stretching, respectively.

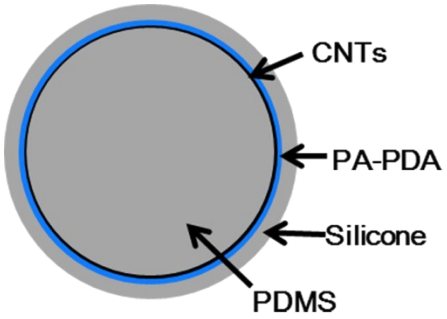

Fig. S4 Schematic illustration for the cross-sectional structure of the electrothermal chromatic fiber.

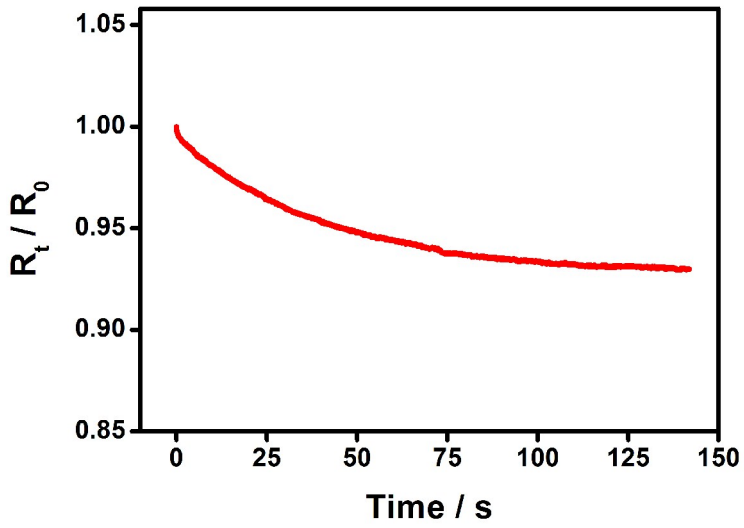

Fig. S5 The evolution of the resistance with time for the composite fiber at a current of 8.1 mA.

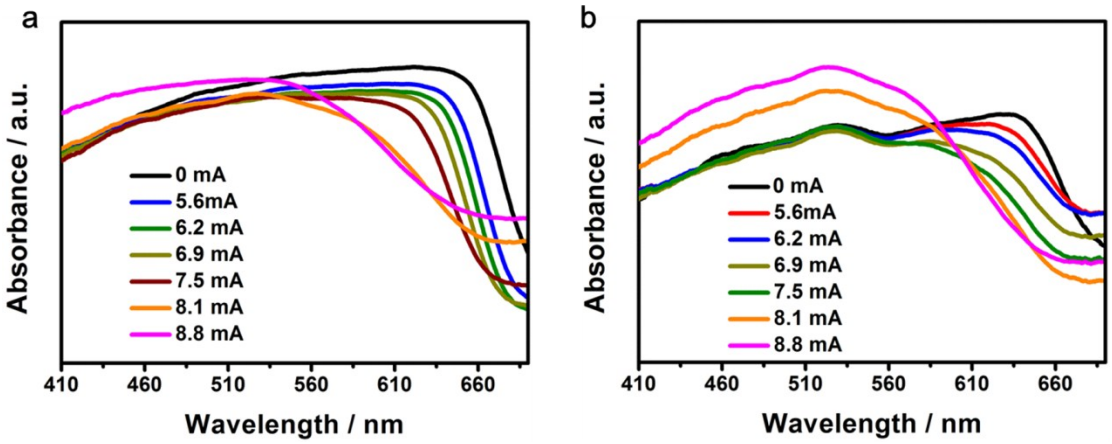

Fig. S6 Electrothermal chromatic performance of the fiber. **a.** UV-vis spectra of the fiber with increasing electric currents at the first cycle. **b.** UV-vis spectra of the fiber at increasing electric currents at the second reversible cycle.

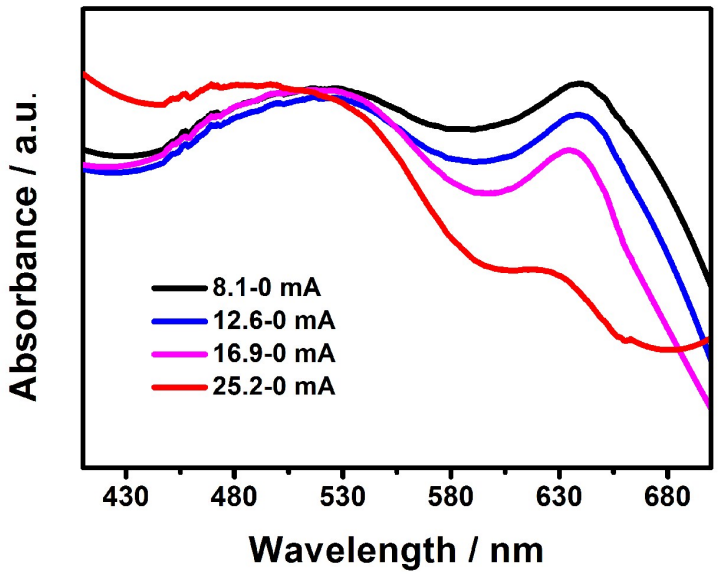

Fig. S7 UV-vis spectra of the electrothermal chromatic fiber after passing with currents of 8.1, 12.6, 16.9 and 25.2 mA.

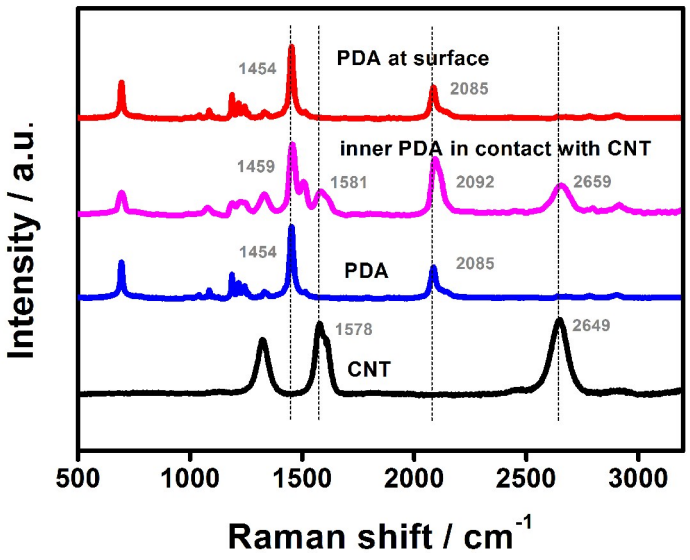

Fig. S8 Raman spectra of different locations in the composite PDA/CNT fiber in comparison to the bare CNT and bare PDA.

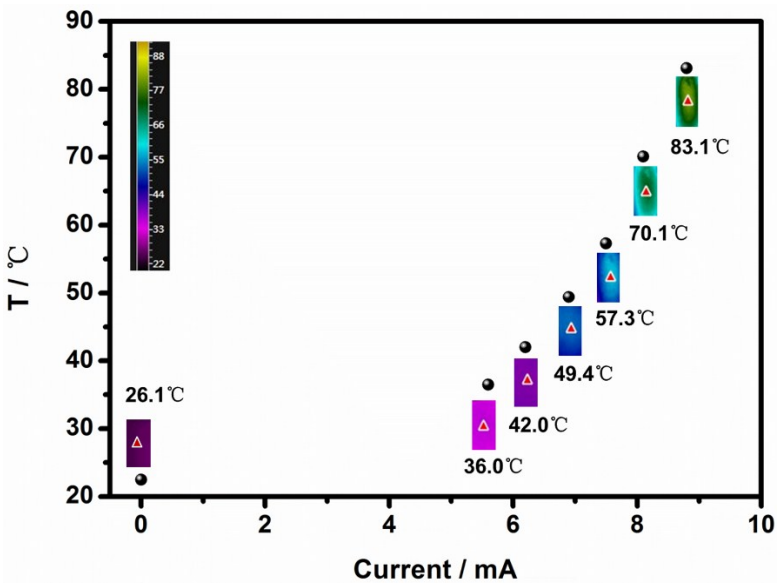

Fig. S9 Temperatures of the composite fiber with increasing electric currents.

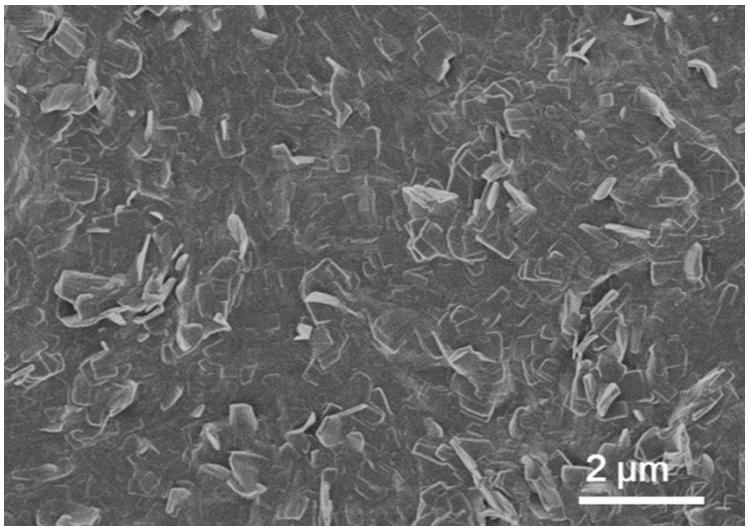

Fig. S10 Morphology transition of bare PDA after a heating and cooling process.

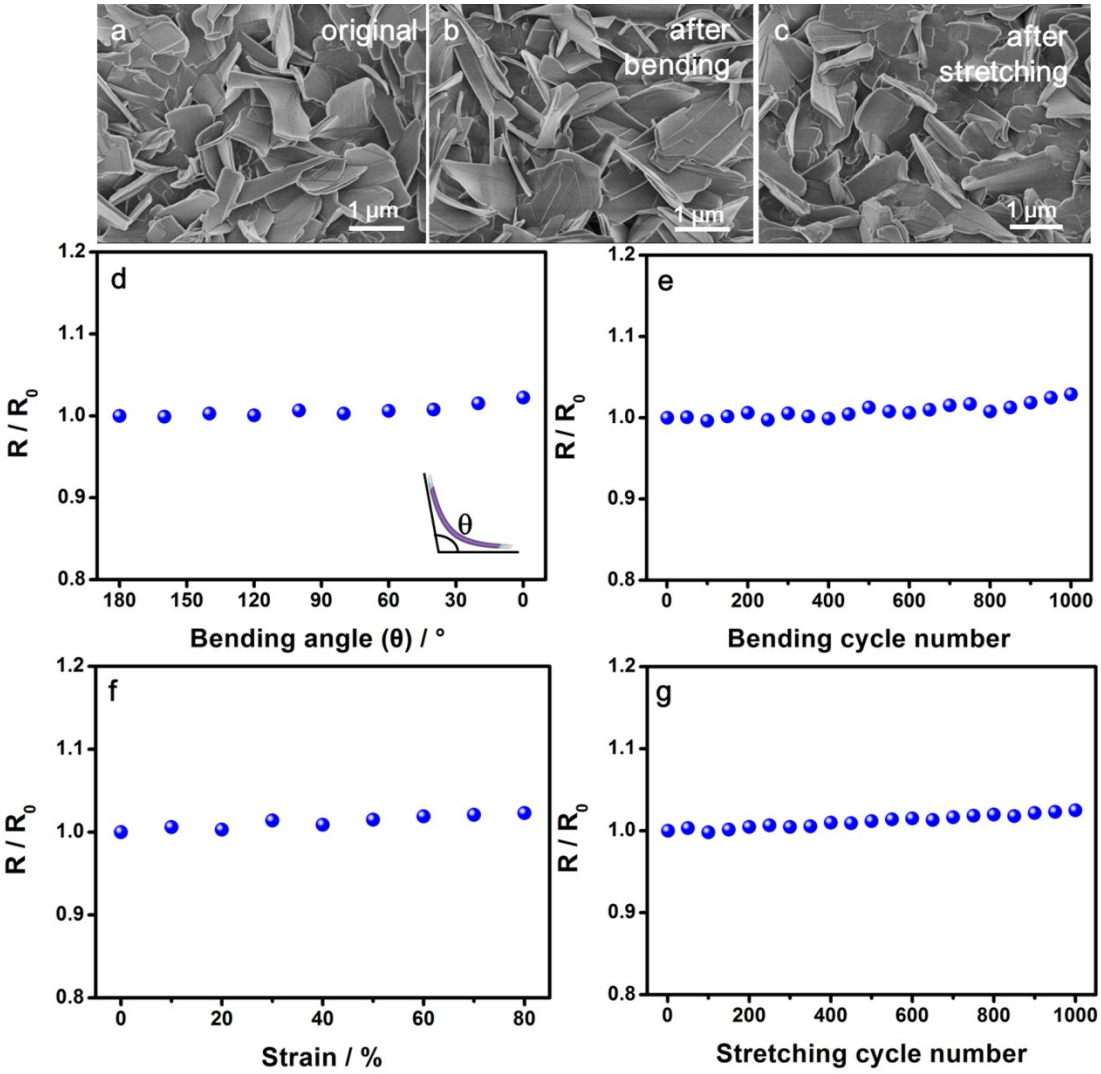

Fig. S11 The evolution in morphology and electrical property of the electrothermal chromatic fiber before and after bending or stretching. **a.** SEM image of an as-synthesized composite fiber. **b.** SEM image after bending. **c**. SEM image after stretching. **d.** Dependence of resistance ratio on bending angle. **e.** Dependence of resistance ratio on bending cycle number (with a bending angle of 90°). **f.** Dependence of resistance ratio on stretching. **g.** Dependence of resistance ratio on stretching cycle number (with a strain of 50%). Here R_0 and R correspond to the resistances before and after bending or stretching, respectively.

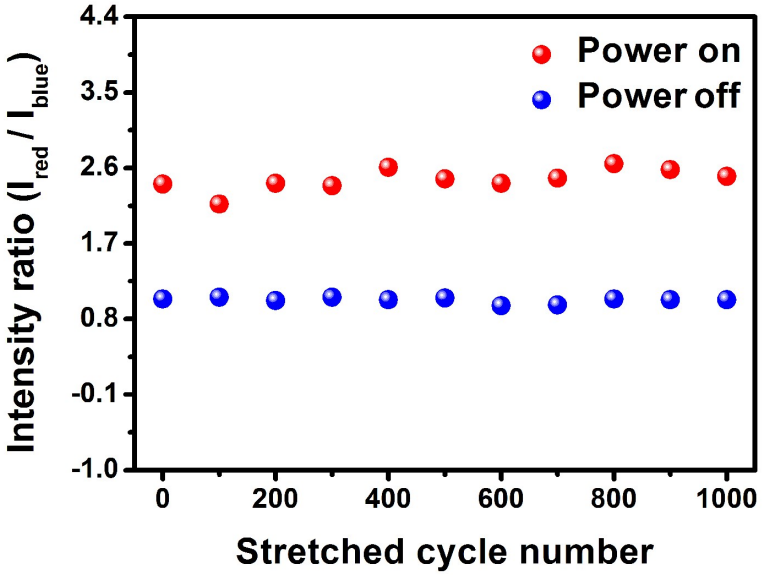

Fig. S12 Intensity ratio of red to blue peaks for a composite fiber being stretched by 50% for 1,000 cycles. The data were collected from UV-vis spectra.

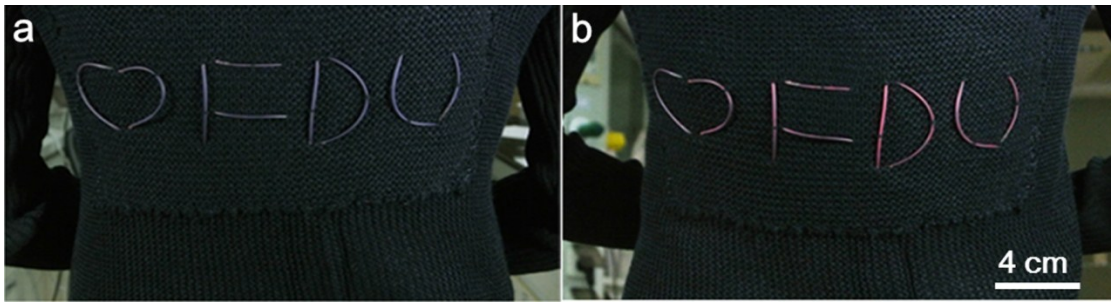

Fig. S13 Electrothermal chromatic fibers being woven into a sweater to display different colors.